Photoinduced Electron Transfer of PAMAM Dendrimer-Zinc(II) Porphyrin Associates at Polarized Liquid|Liquid Interfaces

メタデータ	言語: eng
	出版者:
	公開日: 2017-10-03
	キーワード (Ja):
	キーワード (En):
	作成者:
	メールアドレス:
	所属:
URL	http://hdl.handle.net/2297/43013

Photoinduced Electron Transfer of PAMAM Dendrimer–Zinc(II) Porphyrin Associates at Polarized Liquid|Liquid Interfaces

Hirohisa Nagatani,[*,†] Hiroki Sakae,[‡] Taishi Torikai,[§] Takamasa Sagara[‖] and Hisanori Imura[†]

[†] Faculty of Chemistry, Institute of Science and Engineering, Kanazawa University, Kakuma, Kanazawa 920-1192, Japan

[‡] Division of Material Sciences, Graduate School of Natural Science and Technology, Kanazawa University, Kakuma, Kanazawa 920-1192, Japan

[§] Department of Materials Engineering and Molecular Science, Graduate School of Science and Technology, Nagasaki University, Bunkyo, Nagasaki 852-8521, Japan

[‖] Division of Chemistry and Materials Science, Graduate School of Engineering, Nagasaki University, Bunkyo, Nagasaki 852-8521, Japan

*To whom correspondence should be addressed: H. Nagatani

Tel: +81 76 264 5692; FAX: +81 76 264 6059; E-mail: nagatani@se.kanazawa-u.ac.jp

ABSTRACT

The heterogeneous photoinduced electron transfer reaction of the ion associates between NH$_2$-terminated polyamidoamine (PAMAM) dendrimers and 5,10,15,20-tetrakis(4-sulfonatophenyl)porphyrinato zinc(II) (ZnTPPS^{4-}) was studied at the polarized water|1,2-dichloroethane (DCE) interface. The positive photocurrent arisen from the photoreduction of ZnTPPS^{4-} by a lipophilic quencher, decamethylferrocene, in the interfacial region was significantly enhanced by the ion association with the PAMAM dendrimers. The photocurrent response of the dendrimer–ZnTPPS^{4-} associates was dependent on the pH condition and on generation of dendrimer. A few cationic additives such as polyallylamine and n-octyltrimethyammonium were also examined as alternatives of the PAMAM dendrimer, but the magnitude of the photocurrent enhancement was rather small. The high photoreactivity of the dendrimer–ZnTPPS^{4-} associates was interpreted mainly as a result of the high interfacial concentration of photoreactive porphyrin units associated stably with the dendrimer which was preferably adsorbed at the polarized water|DCE interface. The photochemical data observed in the generation 2 and 4 PAMAM dendrimer systems demonstrated that the higher generation dendrimer which can incorporate a porphyrin molecule more completely in the interior is less efficient for the photocurrent enhancement at the interface. These results indicated that the photoreactivity of ionic reactant at a polarized liquid|liquid interface can readily be modified via ion association with the charged dendrimer.

2

1. INTRODUCTION

The charge transfer and ion partitioning across the interface between two immiscible electrolyte solutions (ITIES) have been studied for separation sciences, pharmacokinetic analysis and mass-transport *in vivo*.[1-2] A heterogeneous photoinduced electron transfer between hydrophilic and lipophilic species at a polarized ITIES has also been investigated as an efficient photo-energy conversion system, because the recombination process of photoproducts isolated in their respective liquid phases is effectively prevented.[3] A variety of porphyrin derivatives heterogeneously react with lipophilic quenchers under the photoexcitation. The photoexcited porphyrin can act as electron donor or acceptor according to the quencher, in which the photocurrent response depends strongly on the adsorption behavior of the porphyrin molecule such as potential-dependent interfacial concentration and molecular orientation. Recent applications of the gold nanoparticles (AuNPs) to the heterogeneous photoinduced electron transfer system demonstrated that the localized surface plasmon (LSP) field generated in the vicinity of AuNPs could improve the photoexcitation efficiency of porphyrin in the interfacial region and, as a result, the photocurrent generation was significantly enhanced.[4-5] The photocurrent intensity generated at dye-sensitized liquid|liquid interfaces is, however, still insufficient and further improvements are required for their practical applications.

Dendrimers are organic nanomaterials capable of molecular capsule or container. A variety of organic molecules and metal ions can be accommodated in the internal cavity through hydrophobic and electrostatic interactions.[6-9] Dendrimers thus have attracted much attention in regard to nanoreactors and drug delivery system.[10-14] Recently, the ion transfer and adsorption behavior of commonly used polyamidoamine (PAMAM) dendrimers have been studied at the polarized water|DCE interface.[15-17] The interfacial mechanism of the dendrimer is considerably affected by the pH condition. The positively charged PAMAM dendrimers are liable to associate with anionic species. The PAMAM dendrimer with NH_2-teminal groups, for instance, can stably incorporate anionic *meso*-substituted porphyrins and protect the porphyrin molecules from the proton attack even under acidic conditions.[18] The spectroelectrochemical analysis elucidated that the molecular encapsulation of anionic species in the

3

PAMAM dendrimer at polarized liquid|liquid interfaces could be controlled as a function of the Galvani potential difference.[19] The photochemical applications of the PAMAM dendrimer have been developed through the formation of nanocomposites with various organic molecules and quantum dots.[20-27] Unique characteristics of these dendrimer-based nanocomposites are comprised of the molecular encapsulation ability as well as improvements of the photostability of dye species and/or reaction yield. The dendrimers have, however, not been applied to the heterogeneous photoreaction at a liquid|liquid interface, where the electron donor and acceptor located in their respective liquid phases can react each other only in the interfacial region under the photoexcitation.

In this study, the photoreactivity of the ion associates between the PAMAM dendrimer and *meso*-sulfonatophenyl substituted zinc(II) porphyrin was studied at the polarized water|DCE interface. The photocurrent response associated with the heterogeneous photoreduction of the water-soluble zinc(II) porphyrin by a lipophilic ferrocene derivative was significantly enhanced by formation of the ion associates.

2. EXPERIMENTAL SECTION

2.1. Reagents. 5,10,15,20-Tetrakis(4-sulfonatophenyl)porphyrinato zinc(II) tetrasodium salt (Na$_4$ZnTPPS) (Frontier Scientific) was used without further purification. The second (G2) and fourth generations (G4) of PAMAM dendrimer with ethylenediamine core were purchased from Aldrich (10 wt% (G4) or 20 wt% (G2) in methanol) and prepared as an aqueous solution after removing methanol by drying in ultra-pure argon gas (>99.999%). Decamethylferrocene (DMFc) (Wako Chemicals, >98%) as a lipophilic quencher was dissolved in the organic phase. The organic solvent, 1,2-dichloroethane (DCE), was of HPLC grade (Nacalai Tesque, 99.7%). The composition of the electrochemical cell was represented in **Figure 1**. The concentration of ZnTPPS^{4-} and the dendrimer in the aqueous phase was 1.0×10^{-5} mol dm^{-3} unless otherwise noted. n-Octyltrimethyammonium bromide (C$_8$TAB) (TCI, >98%) and poly(allylamine hydrochloride) (PAH) (Aldrich, average molecular weight ~58,000) were also examined as alternative additives for the dendrimer. The concentration of C$_8$TAB was 1.0×10^{-5} mol

4

dm^{-3} in the aqueous phase. In the case of a cationic polyelectrolyte, PAH, the weight equal to the G2 PAMAM dendrimer was added into the aqueous phase, i.e., 0.033 g dm^{-3}. The supporting electrolytes were 1.0 × 10^{-2} mol dm^{-3} LiCl for the aqueous phase and 5.0 × 10^{-3} mol dm^{-3} bis(triphenylphosphoranylidene)ammonium terakis(pentafluorophenyl)borate (BTPPATPFB) for the organic phases, respectively. BTPPATPFB was prepared by metathesis of bis(triphenylphosphoranylidene)ammonium chloride (BTPPACl) (Aldrich, 97%) and lithium tetrakis(pentafluorophenyl)borate (LiTPFB) ethyl ether complex (TCI, >70% and Tosoh Finechem, >88%). All other reagents were of analytical grade. The aqueous solutions were prepared with highly purified water from a Milli-Q system (Millipore, 18.2 MΩ cm). The pH of the aqueous phase was controlled by the addition of 5.0 × 10^{-2} mol dm^{-3} LiH$_2$PO$_4$/LiOH for 5.1 ≤ pH ≤ 7.2 and LiOH for pH 12.1, respectively.

| Ag | AgCl | 1.0×10^{-3} mol dm^{-3} BTPPACl 1.0×10^{-2} mol dm^{-3} LiCl (aq) | 1.0×10^{-3} mol dm^{-3} DMFc 5.0×10^{-3} mol dm^{-3} BTPPATPFB (DCE) | **dendrimer ZnTPPS^{4-}** buffer 1.0×10^{-2} mol dm^{-3} LiCl (aq) | AgCl | Ag |

Figure 1. Composition of the electrochemical cell.

2.2. Photoelectrochemical Setup. The photoelectrochemical cell was analogous to one reported previously.[28] The water|DCE interface with a geometrical area of 0.50 cm^2 was polarized by a four-electrode potentiostat (Hokuto Denko, HA1010mM1A). Platinum wires were used as counter electrodes in both aqueous and organic phases. The Luggin capillaries were provided for the reference electrodes (Ag/AgCl) in both phases. The Galvani potential difference ($\Delta_o^w\phi \equiv \phi^w - \phi^o$) was estimated by taking the formal transfer potential ($\Delta_o^w\phi^{o'}$) of tetramethylammonium as 0.160 V.[29] The water|DCE interface was illuminated in total internal reflection (TIR) mode by a cw laser at 410 nm (Neoark, TC20-4030S-2F-4.5).[4] A lock-in detection of ac-photocurrent was performed at 11 Hz by a digital lock-in amplifier with an optical chopper (NF, LI5640 with 5584A). The photocurrent action spectrum was measured by using a Xe lamp (Hamamatsu Photonics, LC8-03, 150 W) with a monochromator (Jobin-Yvon, H10VIS). The

monochromatized excitation light was irradiated perpendicularly to the interface at 3.2 Hz. All the experiments were carried out in a thermostated room at 298 ± 2 K.

2.3. Interfacial Tension Measurements. The electrocapillary curves were obtained from quasi-elastic laser scattering (QELS) measurements with the same cell composition displayed in **Figure 1**. The optical setup and analytical procedure of QELS were reported in detail previously.[30-31] The laser light beam, which passed through the polarized water|DCE interface perpendicularly, was a cw laser at 660 nm (Coherent, CUBE 660-60C, 60 mW). The diffraction grating with 0.320 mm line spacing was placed after the interface. The optical beat of third-order diffraction spot was detected by a Si photodiode (Hamamatsu Photonics, S1133-01) with a wide bandwidth amplifier (Melles Griot, 13AMP005) and was analyzed by a fast-Fourier transform analyzer (Stanford Research Systems, SR770). QELS experiments were carried out in a thermostated room at 293 ± 1 K. The interfacial tension (γ_i) was calculated from the frequency of maximum intensity associated with the mean frequency of the capillary waves.[32-33]

2.4. X-ray Absorption Fine Structure (XAFS) Analysis. The Zn K-edge XAFS spectra of ZnTPPS^{4-} dissolved in the aqueous phase buffered with 5.0×10^{-3} mol dm^{-3} LiH$_2$PO$_4$/LiOH were measured in the fluorescence mode by a 19-element Ge solid state detector (SSD) (Canberra) at Photon Factory, BL12C, Tsukuba, Japan.[34] The XAFS data were analyzed based on a single coordination shell model. The extended X-ray absorption fine structure (EXAFS) for the molecular structure optimized by a Molecular Mechanics (MM) calculation was evaluated *ab initio* using FEFF ver. 8.4.[35] The relative coordination number (*n'*) of zinc atom was estimated by taking the Debye-Waller factor (σ) as 0.075, which was determined for a powder sample of Na$_4$ZnTPPS (5 wt% in a boron nitride pellet) assuming the first coordination shell defined as four equatorial nitrogen atoms. An EXAFS analysis was performed in the *k*-space range from 2.3 to 9.0 Å^{-1}, where *k* is the photoelectron wave vector. The details of the analytical procedure are described elsewhere.[36]

6

3. RESULTS AND DISCUSSION

3.1. Spectroscopic Characterizations of PAMAM Dendrimer–ZnTPPS⁴⁻ Associates. The anionic free base and zinc(II) porphyrins spontaneously form the stable ion associates with the positively charged PAMAM dendrimer in the aqueous solution over a wide pH range.[16, 18] The ion association stability was reported for *meso*-sulfonatophenyl substituted porphyrin (TPPS) compounds as: G4 PAMAM dendrimer−ZnTPPS⁴⁻ > G2 PAMAM dendrimer−ZnTPPS⁴⁻ > G4 PAMAM dendrimer−H₂TPPS⁴⁻ > G2 PAMAM dendrimer−H₂TPPS⁴⁻. The ion association between the anionic porphyrin and the dendrimer is promoted mainly by the electrostatic interaction. In addition, the strong interaction for ZnTPPS⁴⁻ could be interpreted as the axial coordination to the zinc(II) center of the porphyrin molecule by amidoamine branch or tertiary amine of the dendrimer. Typical UV-Vis absorption spectra of ZnTPPS⁴⁻ with the equimolar dendrimers in the aqueous solution are shown in **Figure 2**. The net charge on the PAMAM dendrimer depends on protonation equilibria of primary amines in the periphery moiety ($pK_{a2,den}$ 9.20) and tertiary amines as branch points ($pK_{a1,den}$ 6.65),[37] and hence the dendrimers were positively charged state under experimental conditions (pH ≤ 7). The ion association between the dendrimer and ZnTPPS⁴⁻ was confirmed from the spectral changes in all
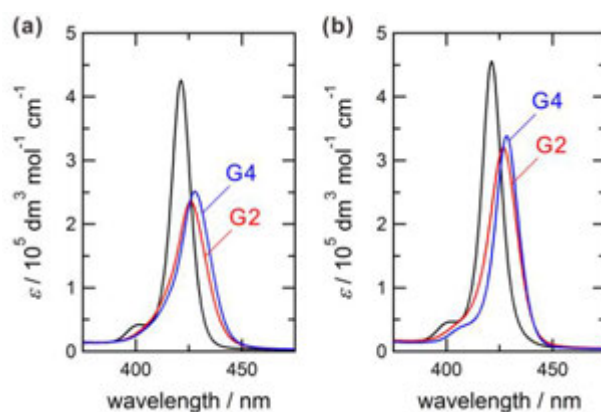
Figure 2. UV-Vis absorption spectra of ZnTPPS⁴⁻ in the presence of the equimolar dendrimer in aqueous solution at (a) pH 5.1–5.4 and (b) pH 7.2. The blue, red and black lines refer to the G4 PAMAM dendrimer–ZnTPPS⁴⁻, G2 PAMAM dendrimer–ZnTPPS⁴⁻ and ZnTPPS⁴⁻ systems, respectively. The concentration of ZnTPPS⁴⁻ and the dendrimers was 1.0×10^{-5} mol dm⁻³.

7
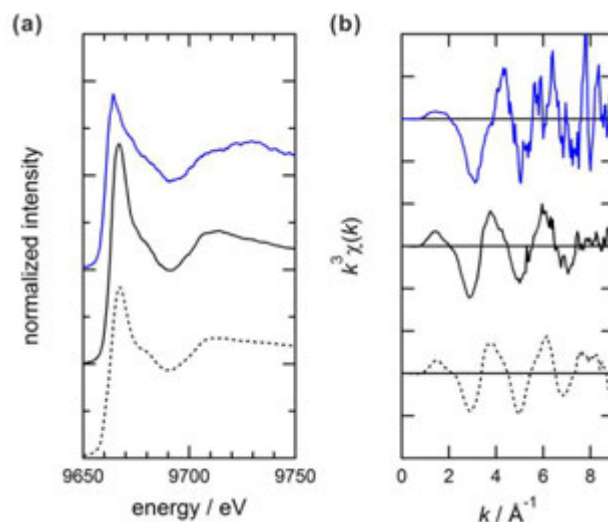
Figure 3. (a) XAFS and (b) $k^3\chi(k)$ spectra for Zn K-edge of ZnTPPS^{4-} measured in the fluorescence mode. The black dashed and solid lines denote the solid powder and 5.6×10^{-4} mol dm^{-3} ZnTPPS^{4-} in aqueous solution at pH 7.1, respectively. The blue line is 7.0×10^{-5} mol dm^{-3} ZnTPPS^{4-} in the presence of the equimolar G4 PAMAM dendrimer at pH 7.9.

examined systems. The absorption maximum wavelength (λ_{max}) at the Soret band of ZnTPPS^{4-} was red-shifted from 421 nm to 428 nm in the presence of the G4 PAMAM dendrimer at pH 5.4 and 7.2. The spectral shifts were slightly less effective with the G2 PAMAM dendrimer, i.e., $\lambda_{max} = 426$ nm at pH 5.2 and 427 nm at pH 7.2. The positive charges on the PAMAM dendrimer are localized on the periphery moiety under neutral conditions, whereas the dendrimer is totally charged in the acidic solution. The relative location of ZnTPPS^{4-} in the ion associate could be influenced by protonation equilibria of the dendrimer.[38] The absorption maximum wavelength of the ion associates was, however, hardly dependent on the pH condition.

In order to characterize the ion association between the PAMAM dendrimer and ZnTPPS^{4-}, the XAFS analysis for the ion associates was carried out in the aqueous solution under neutral conditions. **Figure 3** represents the XAFS and $k^3\chi(k)$ spectra for Zn K-edge of ZnTPPS^{4-} measured in the absence and presence of the equimolar G4 PAMAM dendrimer. The X-ray absorption near-edge structure (XANES) for ZnTPPS^{4-} in the presence of the G4 PAMAM dendrimer was apparently changed in comparison with

the solid powder and aqueous solution samples of ZnTPPS (**Figure 3a**). Since the XANES region is highly sensitive to the coordination geometry, the XAFS spectra indicate that the coordination structure around the zinc atom is modified by the ion association with the dendrimer. The $k^3\chi(k)$ spectra in the EXAFS region also exhibited a certain phase-shift at $k > 3$ Å^{-1} for the G4 PAMAM dendrimer–ZnTPPS^{4-} system (**Figure 3b**). The relative coordination numbers (n') estimated from a curve-fitting based on the single-shell model are summarized in **Table 1**. The additional coordination of amide and tertiary amine nitrogen atoms to the zinc(II) center is responsible for a considerable increase of the n' value for the G4 PAMAM dendrimer–ZnTPPS^{4-} system (n' = 5.1),[9] although the formation of the ion associate results from the electrostatic interaction between protonated amines of the dendrimer and anionic sulfonatophenyl groups of ZnTPPS^{4-} under neutral conditions. The slight increase of the n' value for the ZnTPPS^{4-} system (n' = 4.2) possibly arises from the hydration of ZnTPPS^{4-} in the aqueous solution. The slightly shortened coordination distance (R) for the solution samples should not be discussed quantitatively within the approximate analysis based on the simple single-shell model. In any event, it is evident that both the electrostatic interaction and additional coordination to the zinc(II) center are contributed to the formation of dendrimer–ZnTPPS^{4-} associates.

Table 1. Structural parameters determined by EXAFS analysis[a]

	n'	R / Å	σ / Å
G4–ZnTPPS^{4-} aq. soln.	5.1	2.01	
ZnTPPS^{4-} aq. soln.	4.2	2.01	
ZnTPPS^{4-} (powder)	4	2.03	0.075

[a] n' and R relate to the relative coordination number and the coordination distance, respectively. The Debye-Waller factor (σ) was determined by analyzing the powder sample with n' fixed as 4 and used for the solution samples.

3.2. Photocurrent Responses of Dendrimer–ZnTPPS^{4-} Associates at the Water|DCE Interface. **Figure 4** shows cyclic voltammograms (CVs) measured for the dendrimer–ZnTPPS^{4-} system under dark conditions. Taking into account the acidity constants of terminal amino groups (64 units for G4 and 16 units for G2, p$K_{a2,den}$ 9.20) and interior tertiary amines (62 units for G4 and 14 units for G2, p$K_{a1,den}$ 6.65),[37] the PAMAM dendrimer–ZnTPPS^{4-} associates should have positive net charges at pH ≤ 7. At
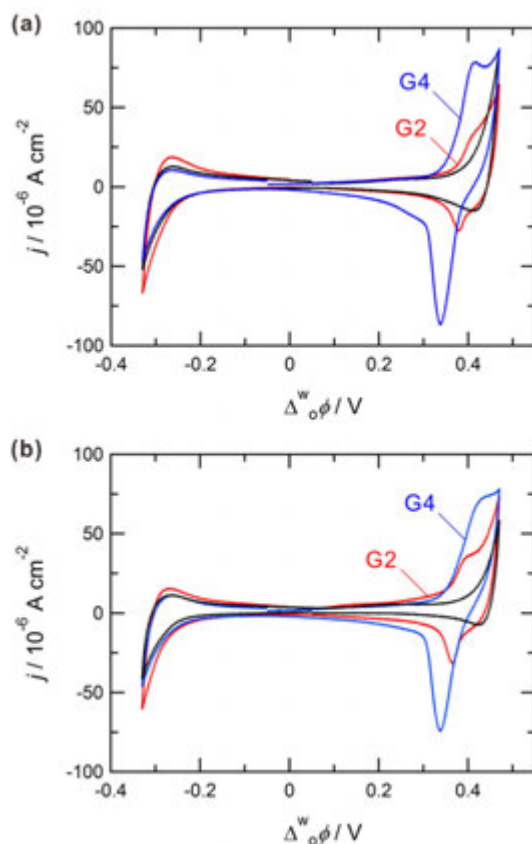
Figure 4. Cyclic voltammograms measured for the dendrimer–ZnTPPS^{4-} systems at (a) pH 5.1–5.4 and (b) pH 7.2. The blue, red and black lines refer to the G4 PAMAM dendrimer–ZnTPPS^{4-}, G2 PAMAM dendrimer–ZnTPPS^{4-} and ZnTPPS^{4-} systems, respectively. The concentrations of ZnTPPS^{4-} with equimolar dendrimers in the aqueous phase and DMFc in the organic phase were 1.0×10^{-5} mol dm^{-3} and 1.0×10^{-3} mol dm^{-3}. The potential sweep rate was 50 mV s^{-1}.

$\Delta_o^w \phi > 0.20\,\text{V}$, the gradual increase of currents was observed in the presence of the dendrimers, which is associated with the ion transfer accompanied by adsorption of the dendrimer and the dendrimer–ZnTPPS^{4-} associate.[16] As reported previously,[18] the voltammetric response for the ion transfer of ZnTPPS^{4-} across the water|DCE interface is negatively shifted from its formal transfer potential $\Delta_o^w \phi_{\text{ZnTPPS}^{4-}}^{\circ\prime} = -0.26\,\text{V}$ by the ion association with the positively charged dendrimer. The slight current increase at the negative edge of the potential window is attributable to the ion transfer of ZnTPPS^{4-} released from the dendrimer. In the present condition, DMFc showed no voltammetric responses within the potential window.

10
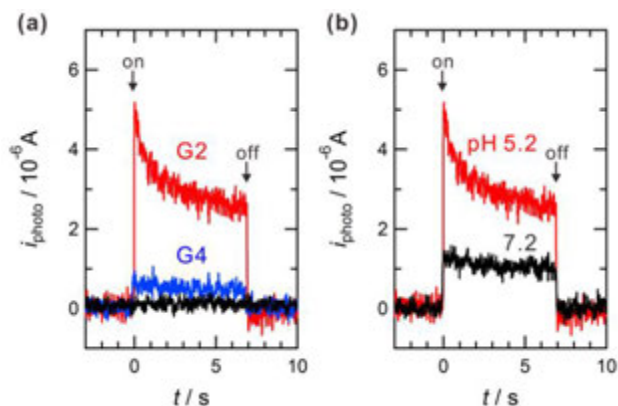
Figure 5. Typical photocurrent transients of ZnTPPS^{4-} at the water|DCE interface in the presence of equimolar dendrimer at 0.20 V. (a) Photocurrent transients measured in the G2 and G4 PAMAM dendrimer–ZnTPPS^{4-} systems at pH 5.2 and 5.4, respectively. The black line refers to the ZnTPPS^{4-} system without adding the dendrimer at pH 5.1. (b) The pH dependence for the G2 PAMAM dendrimer–ZnTPPS^{4-} system.

The photoreactivity of the PAMAM dendrimer–ZnTPPS^{4-} associates was examined at polarized water|DCE interfaces. **Figure 5a** shows typical photocurrent transients in the presence and absence of the dendrimer at pH 5.2–5.4. The photoreactivity of the porphyrin derivatives at a polarized liquid|liquid interface is significantly influenced by their intrinsic redox properties and interfacial behavior. In the heterogeneous photoinduced electron transfer system, ZnTPPS^{4-} is known as a relative inactive dye without forming a specific porphyrin heterodimer,[39-41] although its redox property under photoexcitation is not inferior in comparison with other porphyrin species.[42] The photocurrent response of ZnTPPS^{4-} was, in fact, negligibly small in the absence of the dendrimer. On the other hand, the large positive photocurrent was generated by the PAMAM dendrimers–ZnTPPS^{4-} associates. The photocurrent enhancement by the G2 PAMAM dendrimer was obviously better than that of the G4 PAMAM dendrimer system. In addition, the pH dependence for the G2 PAMAM dendrimer–ZnTPPS^{4-} system shown in **Figure 5b** indicated that larger photocurrents were generated under lower pH conditions (pH < p$K_{a1,den}$, p$K_{a2,den}$) where the terminal primary amines and interior tertiary amines of the dendrimer were almost protonated. It should be noted that no photocurrent was observed for the PMAMA dendrimer

11
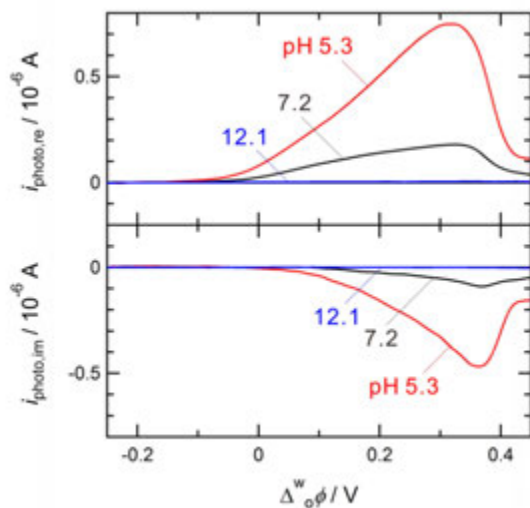
Figure 6. Real ($i_{\mathrm{photo,re}}$) and imaginary ($i_{\mathrm{photo,im}}$) components of the ac-photocurrent for the G2 PAMAM dendrimer–ZnTPPS^{4-} system at various pHs. The photoexcitation frequency was 11 Hz.

alone in the absence of ZnTPPS^{4-}. Since the chemical state of the ZnTPPS^{4-} molecule is identical at pH > 5, the photocurrent enhancement should be attributed to the increase of interfacial concentration of the photoreactive ZnTPPS^{4-} or improvement of electron transfer kinetics in the presence of the dendrimer. The PAMAM dendrimers are effectively adsorbed at the water|DCE interface under acidic conditions,[16] and the interfacial concentration of ZnTPPS^{4-} could be increased through the electrostatic interaction with the positively charged dendrimer. The photocurrent increased immediately in the on-transient from zero to pseudo steady-state values and the fast transient response excludes slow kinetic processes such as the ion transfer of photoproducts.[43-44] The positive photocurrent observed in the present system is, therefore, associated with the heterogeneous electron transfer from the organic phase to the aqueous phase accompanied by the heterogeneous photoreduction of ZnTPPS^{4-} of the ion associates ($\mathrm{D\cdots ZnTPPS}^{4-}$) by DMFc in the interfacial region:

$$\mathrm{D\cdots ZnTPPS}_{\mathrm{w}}^{4-} + \mathrm{DMFc}_{\mathrm{o}} \xrightarrow{\ h\nu\ } \mathrm{D\cdots ZnTPPS}_{\mathrm{w}}^{5-} + \mathrm{DMFc}_{\mathrm{o}}^{+} \qquad (1)$$

where the subscripts w and o refer to the aqueous and organic phases, respectively.

The lock-in detection of the ac-photocurrents under the periodic photoexcitation at 11 Hz was carried out in order to investigate the potential dependence of interfacial photoreactivity of the ion associates.

12

Figure 6 shows the ac-photocurrents measured for the G2 PAMAM dendrimer–ZnTPPS^{4-} system at various pHs. The relatively large ac-photocurrents were observed under acidic and neutral conditions, where the positively charged dendrimers interact preferably with the anionic porphyrin. On the other hand, the ac-photocurrent responses were negligible at pH 12.1. The magnitude of the real ($i_{photore}$) and imaginary ($i_{photoim}$) components of the ac-photocurrent measured at pH 5.3 and 7.2 increased gradually at positive potentials. In our previous study,[18] the interfacial adsorption of positively charged PAMAM dendrimer−ZnTPPS^{4-} associates was observed at positive potentials and ZnTPPS^{4-} was released from the dendrimers at negative potentials. When the ZnTPPS^{4-} anions dissociate from the dendrimer into the bulk aqueous or organic phases, the interfacial concentration of photoreactive ZnTPPS^{4-} decreases drastically and no effective photoreaction takes place at the interface in analogy with the ZnTPPS^{4-} system in the absence of the dendrimer. The apparent photocurrent responses at positive potentials under neutral and acidic conditions therefore result from the photoreduction of ZnTPPS^{4-} units of the ion associates adsorbed at the interface. The photocurrent in the G2 PAMAM dendrimer–ZnTPPS^{4-} system was maximized around 0.32 V and then rapidly decreased at potentials more positive than the ion transfer of the G2 PAMAM dendrimer–ZnTPPS^{4-} associates around 0.35–0.40 V (cf. **Figure 4**). In general, the concentration of a surface-active ion at a polarized liquid|liquid interface is maximized around its transfer potential.[45-46] The large photocurrent observed at ca. 0.32 V close to the transfer potential of the PAMAM dendrimer can correlate with the increase of the interfacial concentration of the dendrimer–ZnTPPS^{4-} associates. In addition, the gradual increase of negative $i_{photoim}$ was observed in the slightly positive potential region than that of maximum $i_{photore}$, where the dendrimer–ZnTPPS^{4-} associates are transferred into the organic phase across the interface, suggesting the participation of slow charge transfer processes involving the ion transfer of photoproducts generated in the homogeneous photoreaction in the organic phase.[43-44]

The photocurrent action spectra were measured to elucidate the wavelength-dependence of the photoreactivity of the dendrimer–ZnTPPS^{4-} associates at the interface. As shown in **Figure 7**, the

13
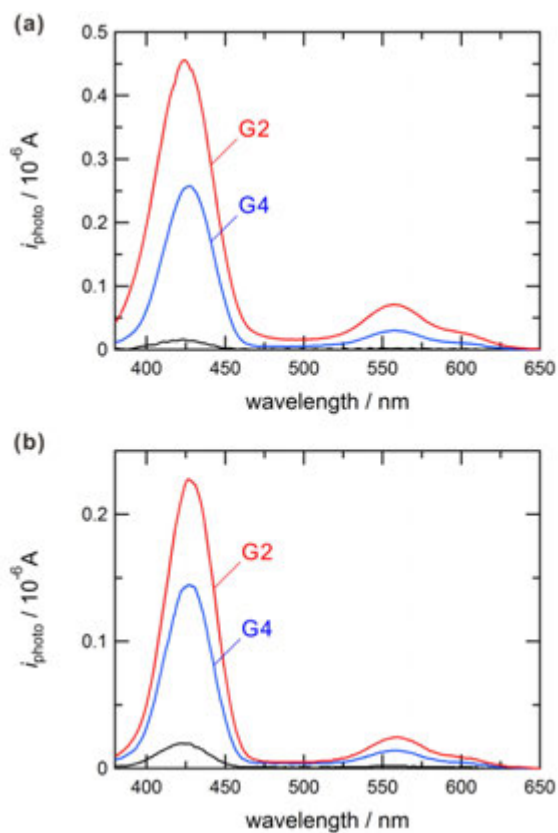
Figure 7. Photocurrent action spectra measured at 0.20 V for the dendrimer–ZnTPPS^{4-} systems at (a) pH 5.1–5.4 and (b) pH 7.2. The blue, red and black lines denote the G4 PAMAM dendrimer–ZnTPPS^{4-}, G2 PAMAM dendrimer–ZnTPPS^{4-} and ZnTPPS^{4-} systems, respectively.

photocurrents were enhanced over the whole visible wavelength in the presence of the dendrimer, especially the G2 PAMAM dendrimer. The spectral shape of the photocurrent action spectra is quite similar to the bulk absorption spectrum measured in the aqueous solution. The photocurrent maximum wavelengths ($\lambda_{i_{photo},max}$) observed under potentiostatic conditions are summarized in **Table 2**. The $\lambda_{i_{photo},max}$ values coincide roughly with the Soret band of ZnTPPS^{4-} in each system. The photocurrent action spectra demonstrated that the photoreactive species at the polarized water|DCE interface were essentially identical to the bulk species in the aqueous solution, i.e., the ion associate without dissociation in the dendrimer–ZnTPPS^{4-} systems.

14

Table 2. Photocurrent maximum wavelengths ($\lambda_{i_{photo},max}$) at the water|DCE interface

	$\lambda_{i_{photo},max}$ / nm					
	pH 5			pH 7		
$\Delta_o^w \phi$ / V	G2–ZnTPPS^{4-}	G4–ZnTPPS^{4-}	ZnTPPS^{4-}	G2–ZnTPPS^{4-}	G4–ZnTPPS^{4-}	ZnTPPS^{4-}
0.20	424	427	423	427	427	423
0.30	423	426	ca.423	427	427	ca.423
bulk aq. phase[a]	425.8	427.8	421.2	426.8	428.4	421.2

[a] The absorption maximum wavelengths measured in the aqueous solution.

3.3. Effects of Cationic Additives for the Photocurrent Generation. As discussed in **Section 3.2**, the high photoreactivity of the dendrimer–ZnTPPS^{4-} associates could be correlated with the potential-dependent adsorption behavior where the interfacial concentration is increased around 0.35–0.40 V. The electrostatic ion associations between anionic porphyrins and surface active cations have been reported in solutions and at liquid|liquid interfaces.[31, 47-48] A few cationic additives, C$_8$TAB and PAH, were examined as alternatives of the PAMAM dendrimer for the photocurrent enhancement at the polarized interface. The adsorption behavior of the water-soluble additives at polarized water|DCE interfaces was evaluated from the electrocapillary curves measured by means of QELS (**Figure 8**). The significant decreases of γ_i were observed in the presence of the dendrimers, in which the G4 PAMAM dendrimer
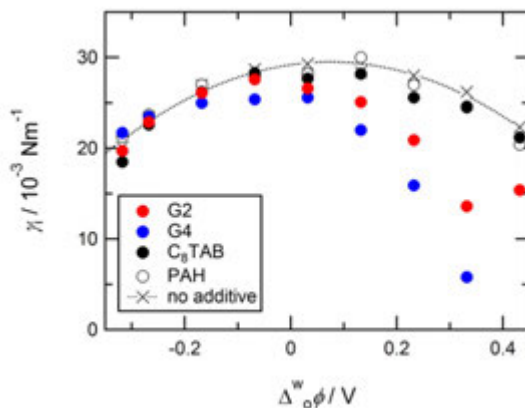
Figure 8 Electrocapillary curves measured for cationic additives at pH 7.2. The concentrations were 1.0×10^{-5} mol dm^{-3} for ZnTPPS^{4-}, the dendrimers and C$_8$TAB, and 0.033 g dm^{-3} for PAH, respectively.

indicated the strong adsorption property at positive potentials. The γ_i values for the G2 PAMAM dendrimer showed the minimum value around 0.33 V close to its transfer potential. On the other hand, C$_8$TAB and PAH exhibited rather weak effects. Although the formal transfer potential of n-octyltrimethylammonium cation (C$_8$TA$^+$) was determined as $\Delta_o^w \phi_{C_8TA^+}^{o'} = -0.11\,\text{V}$ from the CV measurements, no significant decrease in interfacial tension was observed around $\Delta_o^w \phi_{C_8TA^+}^{o'}$ under the present experimental condition. The degree of adsorption at the water|DCE interface was found as: G4 PAMAM dendrimer > G2 PAMAM dendrimer >> C$_8$TAB, (PAH).

Figure 9 shows the ac-photocurrent responses at pH 7.2 in the presence of the cationic additives. Among the additives examined in this study, the dendrimers induced large photocurrents. PAH also indicated certain effects on the photocurrent enhancement, whereas the photocurrent intensity of the
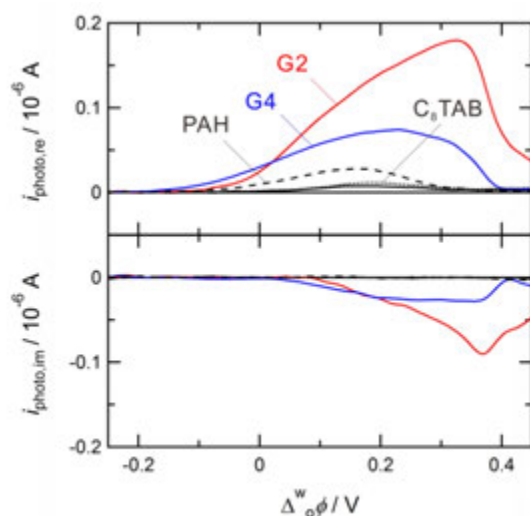
Figure 9 Potential dependence of the real ($i_{\text{photo,re}}$) and imaginary ($i_{\text{photo,im}}$) components of the ac-photocurrent at pH 7.2. The blue, red and black solid lines denote the G4 PAMAM dendrimer–ZnTPPS^{4-}, G2 PAMAM dendrimer–ZnTPPS^{4-} and ZnTPPS^{4-} systems, respectively. The dotted and dashed lines are the C$_8$TAB–ZnTPPS^{4-} and PAH–ZnTPPS^{4-} systems, respectively. The concentrations were 1.0×10^{-5} mol dm^{-3} for ZnTPPS^{4-}, the dendrimers and C$_8$TAB, and 0.033 g dm^{-3} for PAH, respectively.

C$_8$TAB–ZnTPPS^{4-} system was practically the same as that of the ZnTPPS^{4-} system. At pH 7.2, the positively charged polyallylamine, whose pK_a of amine groups is 8.7,[49] could be associated with ZnTPPS^{4-} anions, although no spectral shift of the absorption bands of ZnTPPS^{4-} in the presence of PAH was indicative of weak interactions in the bulk aqueous phase. The relative magnitudes of i_{photore} at 0.20 V were ca. 3.5 (PAH), 10 (G4 PAMAM dendrimer) and 20 times (G2 PAMAM dendrimer) larger than the ZnTPPS^{4-} system. Taking into account the adsorption of the ion associates involving ZnTPPS^{4-} which increases the interfacial concentration of the photoreactant, the potential dependences of the photocurrent measured in the dendrimer–ZnTPPS^{4-} systems were roughly consistent with the interfacial tension lowering shown in **Figure 8**. The effective photocurrent generation was observed in the dendrimer–ZnTPPS^{4-} systems at potentials where the γ_i values decreased, i.e., $\Delta_o^w \phi \geq -0.1\,\mathrm{V}$ (G2 PAMAM dendrimer) and $\Delta_o^w \phi \geq -0.2\,\mathrm{V}$ (G4 PAMAM dendrimer). The relatively large effect by the G2 PAMAM dendrimer could be correlated with the preferable incomplete encapsulation of ZnTPPS^{4-}. The Gibbs free energies of ion association between the dendrimers and ZnTPPS^{4-} ($\Delta G_{\mathrm{D\cdots ZnP}}$) at the polarized water|DCE interface were reported respectively as -18.3 ± 0.5 kJ mol^{-1} for the G2 PAMAM dendrimer and -30.1 ± 0.9 kJ mol^{-1} for the G4 PAMAM dendrimer at pH 7.2.[18] The $\Delta G_{\mathrm{D\cdots ZnP}}$ values indicate explicitly a high stability of the G4 PAMAM dendrimer–ZnTPPS^{4-} associate. The ZnTPPS^{4-} molecule can penetrate into the interior of the larger spherical G4 PAMAM dendrimer, while ZnTPPS^{4-} associated with the small flat-elliptical G2 PAMAM dendrimer is exposed to the outer solution phase. The effective inhibition of the protolytic demetalation of ZnTPPS^{4-} has also been attained even under acidic conditions by the G4 PAMAM dendrimer but not by the G2 PAMAM dendrimer. These findings indicate that the ZnTPPS^{4-} molecule completely incorporated in the higher generation dendrimer seems not to react readily with DMFc located in the organic phase. In spite of higher interfacial concentration expected for the G4 PAMAM dendrimer–ZnTPPS^{4-} associate from the electrocapillary curves in **Figure 8**, as a result, the heterogeneous electron transfer from DMFc to ZnTPPS^{4-} incorporated in the G4

17

PAMAM dendrimer at the interface was less efficient than the G2 PAMAM dendrimer–ZnTPPS^{4-} system.

4. CONCLUSIONS

The photoreactivity of the PAMAM dendrimer–ZnTPPS^{4-} associates was studied at the polarized water|DCE interface. Although the small positive photocurrent is generated intrinsically from the heterogeneous photoreduction of ZnTPPS^{4-} by DMFc at the interface, the photocurrent response was drastically enhanced by the formation of the ion associate with the dendrimer. A certain photocurrent enhancement was also observed in the PAH–ZnTPPS^{4-} system, but not in C$_8$TAB–ZnTPPS^{4-} system. The high photoreactivity of the ion associates can be interpreted from the apparent increase of the interfacial concentration of ZnTPPS^{4-} associated with the surface active cation. Indeed, the PAMAM dendrimers were strongly adsorbed at the polarized water|DCE interface, where the significant photocurrent enhancement and interfacial tension lowering were observed in the same potential region. In addition, the larger photocurrent enhancement in the G2 PAMAM dendrimer–ZnTPPS^{4-} system demonstrated that the higher generation G4 PAMAM dendrimer which can incorporate the ZnTPPS^{4-} molecule more completely is less efficient for the heterogeneous photoreaction system. The results indicate that the interfacial mechanism involving ionic reactants can readily be modified via ion association with the charged dendrimer. This strategy would provide a simple solution for the application of a variety of non-surface active dye species which have ideal redox property for the heterogeneous reaction system without complex chemical modifications.

18

research. The authors are indebted to Dr. Hajime Tanida of Japan Synchrotron Radiation Research Institute (JASRI) for his contributions in the XAFS experiments performed under the approval of the Photon Factory Program Advisory Committee (No. 2007G141).

REFERENCES

1. Watarai, H.; Teramae, N.; Sawada, S. *Interfacial Nanochemistry*. Kluwer Academic/Plenum Publishers: New York, 2005.

2. Volkov, A. G. *Liquid Interfaces in Chemical, Biological, and Pharmaceutical Application*. Marcel Dekker: New York, 2001.

3. Samec, Z.; Eugster, N.; Fermin, D. J.; Girault, H. H. A generalised model for dynamic photocurrent responses at dye-sensitised liquid/liquid interfaces. *J. Electroanal. Chem.* **2005,** *577* (2), 323-337.

4. Nagatani, H.; Tonari, S.; Shibata, T.; Sagara, T. Gold nanoparticles-enhanced photocurrent at a dye-sensitized liquid|liquid interface. *Electrochem. Commun.* **2011,** *13* (9), 985-988.

5. Schaming, D.; Hojeij, M.; Younan, N.; Nagatani, H.; Lee, H. J.; Girault, H. H. Photocurrents at polarized liquid|liquid interfaces enhanced by a gold nanoparticle film. *Phys. Chem. Chem. Phys.* **2011,** *13* (39), 17704-17711.

6. Morgan, M. T.; Carnahan, M. A.; Immoos, C. E.; Ribeiro, A. A.; Finkelstein, S.; Lee, S. J.; Grinstaff, M. W. Dendritic Molecular Capsules for Hydrophobic Compounds. *J. Am. Chem. Soc.* **2003,** *125* (50), 15485-15489.

7. Kannaiyan, D.; Imae, T. PH-Dependent encapsulation of pyrene in PPI-Core:PAMAM-shell dendrimers. *Langmuir* **2009,** *25* (9), 5282-5285.

8. Scott, R. W. J.; Wilson, O. M.; Crooks, R. M. Synthesis, characterization, and applications of dendrimer-encapsulated nanoparticles. *J. Phys. Chem. B* **2005,** *109* (2), 692-704.

9. Tran, M. L.; Gahan, L. R.; Gentle, I. R. Structural studies of copper(II)-amine terminated dendrimer complexes by EXAFS. *J. Phys. Chem. B* **2004,** *108* (52), 20130-20136.

10.   Shi, X.; Majoros, I. J.; Baker Jr, J. R. Capillary electrophoresis of poly(amidoamine) dendrimers: From simple derivatives to complex multifunctional medical nanodevices. *Mol. Pharm.* **2005,** *2* (4), 278-294.

11.   Myers, V. S.; Weir, M. G.; Carino, E. V.; Yancey, D. F.; Pande, S.; Crooks, R. M. Dendrimer-encapsulated nanoparticles: New synthetic and characterization methods and catalytic applications. *Chem Sci* **2011,** *2* (9), 1632-1646.

12.   Svenson, S.; Tomalia, D. A. Dendrimers in biomedical applications - Reflections on the field. *Adv. Drug Delivery Rev.* **2005,** *57* (15), 2106-2129.

13.   Vögtle, F.; Gestermann, S.; Hesse, R.; Schwierz, H.; Windisch, B. Functional dendrimers. *Prog. Polym. Sci.* **2000,** *25* (7), 987-1041.

14.   Nanjwade, B. K.; Bechra, H. M.; Derkar, G. K.; Manvi, F. V.; Nanjwade, V. K. Dendrimers: Emerging polymers for drug-delivery systems. *Eur. J. Pharm. Sci.* **2009,** *38* (3), 185-196.

15.   Berduque, A.; Scanlon, M. D.; Collins, C. J.; Arrigan, D. W. M. Electrochemistry of Non-Redox-Active Poly(propylenimine) and Poly(amidoamine) Dendrimers at Liquid-Liquid Interfaces. *Langmuir* **2007,** *23* (13), 7356-7364.

16.   Nagatani, H.; Ueno, T.; Sagara, T. Spectroelectrochemical analysis of ion-transfer and adsorption of the PAMAM dendrimer at a polarized liquid|liquid interface. *Electrochim. Acta* **2008,** *53* (22), 6428-6433.

17.   González-Fuentes, M. A.; Manríquez, J.; Antaño-López, R.; Godínez, L. A. Electrochemically driven transfer of carboxyl-terminated PAMAM dendrimers at the water/dichloroethane interface. *Electrochem. Commun.* **2010,** *12* (1), 137-139.

18.   Sakae, H.; Nagatani, H.; Morita, K.; Imura, H. Spectroelectrochemical characterization of dendrimer-porphyrin associates at polarized liquid|liquid interfaces. *Langmuir* **2014,** *30* (3), 937-945.

19.   Nagatani, H.; Sakamoto, T.; Torikai, T.; Sagara, T. Encapsulation of anilinonaphthalenesulfonates in carboxylate-terminated PAMAM dendrimer at the polarized water|1,2-dichloroethane interface. *Langmuir* **2010,** *26* (22), 17686-17694.

20. Ogasawara, S.; Ikeda, A.; Kikuchi, J. I. Positive dendritic effect in DNA/porphyrin composite photocurrent generators containing dendrimers as the stationary phase. *Chem. Mater.* **2006,** *18* (25), 5982-5987.

21. Perez-Tejeda, P.; Prado-Gotor, R.; Grueso, E. M. Electrochemiluminescence of the $[Ru(bpy)_3]^{2+}$ complex: The coreactant effect of PAMAM dendrimers in an aqueous medium. *Inorg. Chem.* **2012,** *51* (20), 10825-10831.

22. Zheng, J.; Petty, J. T.; Dickson, R. M. High quantum yield blue emission from water-soluble Au8 nanodots. *J. Am. Chem. Soc.* **2003,** *125* (26), 7780-7781.

23. Lemon, B. I.; Crooks, R. M. Preparation and characterization of dendrimer-encapsulated CdS semiconductor quantum dots [12]. *J. Am. Chem. Soc.* **2000,** *122* (51), 12886-12887.

24. Ghosh, S.; Khan, A. H.; Acharya, S. Fabrication of highly stable, hybrid PbS nanocomposites in PAMAM dendrimer matrix for photodetection. *J. Phys. Chem. C* **2012,** *116* (10), 6022-6030.

25. Kruth, A.; Quade, A.; Brüser, V.; Weltmann, K. D. Plasma-enhanced synthesis of poly(allylamine)-encapsulated ruthenium dye-sensitized titania photocatalysts. *J. Phys. Chem. C* **2013,** *117* (8), 3804-3811.

26. Kim, Y.; Kim, J. Modification of indium tin oxide with dendrimer-encapsulated nanoparticles to provide enhanced stable electrochemiluminescence of $Ru(bpy)_3^{2+}$/tripropylamine while preserving optical transparency of indium tin oxide for sensitive electrochemiluminescence-based analyses. *Anal. Chem.* **2014,** *86* (3), 1654-1660.

27. Bronstein, L. M.; Shifrina, Z. B. Dendrimers as encapsulating, stabilizing, or directing agents for inorganic nanoparticles. *Chem. Rev.* **2011,** *111* (9), 5301-5344.

28. Nagatani, H.; Sagara, T. Pontential-Modulation Spectroscopy at Solid/Liquid and Liquid/Liquid Interfaces. *Anal. Sci.* **2007,** *23* (9), 1041-1048.

29. Wandlowski, T.; Mareček, V.; Samec, Z. Galvani potential scales for water-nitrobenzene and water-1,2-dichloroethane interfaces. *Electrochim. Acta* **1990,** *35* (7), 1173-1175.

30.   Nagatani, H.; Samec, Z.; Brevet, P.-F.; Fermín, D. J.; Girault, H. H. Adsorption and aggregation of meso-tetrakis(4-carboxyphenyl)porphyrinato zinc(II) at the polarized water|1,2-dichloroethane interface. *J. Phys. Chem. B* **2003,** *107* (3), 786-790.

31.   Nagatani, H.; Tanida, H.; Harada, M.; Asada, M.; Sagara, T. Polarized total-reflection X-ray absorption fine structure of zinc(II) porphyrin at the heptane-water interface. *J. Phys. Chem. C* **2010,** *114* (43), 18583-18587.

32.   Langevin, D. *Light Scattering by Liquid Surfaces and Complementary Techniques*. Marcel Dekker: New York, 1992; p 89-104.

33.   Lamb, H. *Hydrodynamics*; Sixth ed.; Dover: New York, 1945. p 457.

34.   Nomura, M. Design and performance of a multi-element SSD for fluorescent XAFS. *KEK Rep.* **1998,** *98-4*, 1-28.

35.   Ankudinov, A. L.; Ravel, B.; Rehr, J. J.; Conradson, S. D. Real-space multiple-scattering calculation and interpretation of x-ray-absorption near-edge structure. *Phys. Rev. B* **1998,** *58* (12), 7565-7576.

36.   Nagatani, H.; Tanida, H.; Watanabe, I.; Sagara, T. Extended X-ray absorption fine structure of copper(II) complexes at the air-water interface by a polarized total-reflection X-ray absorption technique. *Anal. Sci.* **2009,** *25* (4), 475-480.

37.   Leisner, D.; Imae, T. Polyelectrolyte Behavior of an Interpolyelectrolyte Complex Formed in Aqueous Solution of a Charged Dendrimer and Sodium Poly(L-glutamate). *J. Phys. Chem. B* **2003,** *107* (47), 13158-13167.

38.   Paulo, P. M. R.; Costa, S. M. B. Non-covalent dendrimer-porphyrin interactions: The intermediacy of H-aggregates? *Photochem. Photobiol. Sci.* **2003,** *2* (5), 597-604.

39.   Fermín, D. J.; Duong, H. D.; Ding, Z.; Brevet, P. F.; Girault, H. H. Photoinduced electron transfer at liquid/liquid interfaces. Part III. Photoelectrochemical responses involving porphyrin ion pairs. *J. Am. Chem. Soc.* **1999,** *121* (43), 10203-10210.

40.   Eugster, N.; Fermín, D. J.; Girault, H. H. Photoinduced electron transfer at liquid/liquid interfaces. Part VI. On the thermodynamic driving force dependence of the phenomenological electron-transfer rate constant. *J Phys Chem B* **2002,** *106* (13), 3428-3433.

41.   Eugster, N.; Fermín, D. J.; Girault, H. H. Photoinduced electron transfer at liquid/liquid interfaces: Dynamics of the heterogeneous photoreduction of quinones by self-assembled porphyrin ion pairs. *J. Am. Chem. Soc.* **2003,** *125* (16), 4862-4869.

42.   Kalyanasundaram, K.; Neumann-Spallart, M. Photophysical and redox properties of water-soluble porphyrins in aqueous media. *J. Phys. Chem.* **1982,** *86* (26), 5163-5169.

43.   Nagatani, H.; Dejima, S.; Hotta, H.; Ozeki, T.; Osakai, T. Photoinduced electron transfer of 5,10,15,20-tetraphenylporphyrinato zinc(II) at the polarized water/1,2-dichloroethane interface. *Anal. Sci.* **2004,** *20* (11), 1575-1579.

44.   Osakai, T.; Muto, K. Ion transfer and photoinduced electron transfer of water- soluble porphyrin at the nitrobenzene vertical bar water interface. *J. Electroanal. Chem.* **2001,** *496* (1-2), 95-102.

45.   Nagatani, H.; Fermín, D. J.; Girault, H. H. A kinetic model for adsorption and transfer of ionic species at polarized liquid|liquid interfaces as studied by potential modulated fluorescence spectroscopy. *J. Phys. Chem. B* **2001,** *105* (39), 9463-9473.

46.   Kakiuchi, T. Potential-dependent adsorption and partitioning of ionic components at a liquid|liquid interface. *J. Electroanal. Chem.* **2001,** *496*, 137-142.

47.   Fujiwara, K.; Wada, S.; Monjushiro, H.; Watarai, H. Ion-association aggregation of an anionic porphyrin at the liquid/liquid interface studied by second harmonic generation spectroscopy. *Langmuir* **2006,** *22* (6), 2482-2486.

48.   Maiti, N. C.; Mazumdar, S.; Periasamy, N. J- and H-aggregates of porphyrin - Surfactant complexes: Time-resolved fluorescence and other spectroscopic studies. *J. Phys. Chem. B* **1998,** *102* (9), 1528-1538.

49.   Fang, M. Layer-by-layer growth and condensation reactions of niobate and titanoniobate thin films. *Chem. Mater.* **1999,** *11* (6), 1526-1532.

table of contents only